Aerotaxis and aerokinesis of *Dictyostelium discoideum* under hypoxic microenvironments

S. Hirose, J.-P. Rieu, C. Anjard, O. Cochet-Escartin, H. Kikuchi, K. Funamoto

Abstract— Although spatiotemporal changes of oxygen in a microenvironment are known to affect the cellular dynamics of various eukaryotes, the details are not fully understood. Here, we describe the aerotaxis and aerokinesis of *Dictyostelium discoideum* (*Dd*), which has long been employed as a model organism for eukaryotic cells. We developed a microfluidic device capable of time-lapse observation of cultured cells while controlling oxygen concentrations in microchannels. Migratory behaviors of *Dd* were observed and quantitatively evaluated under an oxygen concentration gradient from 0% to 21% O_2, as well as in various uniform oxygen conditions. In a hypoxic region within the oxygen concentration gradient, *Dd* migrated toward regions of higher oxygen concentration at increased velocity, which was independent of cell density. Observed under uniform oxygen concentrations of 1%, 2%, 3%, and 21%, the migration velocity of *Dd* increased significantly in hypoxic environments of 2% O_2 or less. Thus, *Dd* shows aerotaxis, directed by the oxygen concentration gradient, and simultaneously shows aerokinesis, changing the migration velocity according to the oxygen concentration itself.

I. INTRODUCTION

Changes in the oxygen environment are known to affect cellular dynamics *in vivo*. For example, when oxygen conditions in *in vivo* tissues are changed locally by disease or inflammation, or by proliferation or metastasis of cancer cells [1], angiogenesis by vascular endothelial cells [2] and the aggregation of leukocytes [3] are induced. However, such oxygen-dependent changes in cell behaviors and their cellular mechanisms are not fully elucidated. Challenges for elucidating them include the biological complexity of the cells and the difficulty of measuring and controlling *in vivo* oxygen concentrations.

Dictyostelium discoideum (*Dd*) [4] has long been employed as a typical model organism for eukaryotic cell motility. While *Dd* is biologically simple, it has genes that are fundamentally similar to those of mammalian cells [5]. In addition, it has been reported that *Dd* amoebas have some common taxis response characteristics with mammalian cells. For instance, the chemotaxis of *Dd* against chemical factors is reportedly similar to that of polymorphonuclear leukocytes, including the underlying biochemical mechanisms [6]. Moreover, *Dd* has been reported to sense hypoxic conditions [7] by an oxygen-sensing mechanism similar to that of mammalian cells[8]. Therefore, *Dd* is promising as a model for studying taxis responses to oxygen (aerotaxis) and oxygen-dependent motility (aerokinesis).

In this study, we investigated aerotaxis and aerokinesis of *Dd* by using microfluidic devices. The application of microfluidic devices to cellular experiments enables strict controls of microenvironments and a real-time observation of the cultured cells. We have developed such microfluidic devices to precisely and rapidly control oxygen concentration in a microenvironment [9]. The migratory characteristics of *Dd* were clarified by observing them under an oxygen concentration gradient from 0% to 21% and under uniform oxygen concentrations.

II. METHODS

A. Microfluidic Device

We developed a double-layer microfluidic device to control oxygen concentrations in cell-cultured microchannels (Fig. 1). The oxygen concentration inside the device was controlled by supplying gas mixtures at predefined oxygen concentrations into the gas channels and exchanging gases between the gas and media channels. The microfluidic device is 30 × 30 mm square and 3 mm thick, and all channels are 2 mm wide and 150 μm high. The two gas channels with a 1 mm interval are located at 500 μm from the bottom surface, crossing above the three parallel media channels on the bottom. The channel patterns in the device were fabricated from polydimethylsiloxane (PDMS, Sylgard 184 Silicone Elastomer Kit, The Dow Chemical Company, USA) by soft lithography. To create the gas channels, a gas channel-patterned PDMS layer of 2.5 mm thickness was stacked on a media channel-patterned PDMS layer of 0.5 mm thickness after hydrophilization using a plasma cleaner (PDC-32G, Harrick Plasma, USA). Here, a polycarbonate film of 0.5 mm thickness with low gas permeability was embedded inside the gas layer at 0.5 mm above the bottom surface of the gas channels to prevent oxygen infusion from the atmosphere. Then, the bottom surface of the PDMS mold and a glass coverslip of 30 × 30 mm square were also bonded together to create the media channels. By seeding cells into the three media channels, three cellular experiments under the same oxygen condition can be performed simultaneously.

The oxygen concentration inside the device was computed by three-dimensional numerical simulation by commercial finite element software (COMSOL Multiphysics ver. 5.5,

S. Hirose is with the Graduate School of Biomedical Engineering, Tohoku University, Sendai, Japan (email: satomi.hirose.q5@dc.tohoku.ac.jp).

J.-P. Rieu is with the Institute of Light and Matter, Claude Bernard University Lyon 1, Villeurbanne, France (e-mail: jean-paul.rieu@univ-lyon1.fr).

C. Anjard is with the Institute of Light and Matter, Claude Bernard University Lyon 1 (e-mail: christophe.anjard@univ-lyon1.fr).

O. Cochet-Escartin is with the Institute of Light and Matter, Claude Bernard University Lyon 1 (e-mail: Cochet-Escartin@univ-lyon1.fr).

H. Kikuchi is with the Graduate School of Pharmaceutical Sciences, Tohoku University, Sendai, Japan (email: hal@mail.pharm.tohoku.ac.jp).

K. Funamoto is with the Institute of Fluid Science, Tohoku University, Sendai, Japan (corresponding author to provide phone: +81-22-217-5878; fax: +81-22-217-5878; e-mail: funamoto@tohoku.ac.jp).

COMSOL AB, Sweden). The gas mixtures supplied to the gas channels were assumed to be an incompressible fluid with a density of 1×10^3 kg/m^3 and a viscosity of 1×10^{-3} Pa·s. The Navier-Stokes equations and the equation of continuity were solved for the gas flow in the gas channels. As for the boundary conditions of the gas flow analysis, a constant flow rate of 30 ml/min was set at the inlets of the gas channels, and zero pressure was assumed at the outlets. A no-slip condition was applied on the channel wall. Then, spatial distributions of oxygen concentration in the device were computed by solving the convection-diffusion equation. The device was assumed to be surrounded by an atmosphere containing 21% O$_2$, and the initial conditions of oxygen concentration for PDMS, PC, and media were given according to Henry's law. For the interface between PDMS and media, a partition condition was applied to satisfy the continuity of partial pressure of oxygen considering the solubility of oxygen in each substance. A no-flux condition was applied on the glass coverslip on the bottom of the device. In cases where gas mixtures containing 0% and 21% O$_2$ were supplied to the left and right gas channels, respectively, an oxygen concentration gradient from 0.4% to 21% O$_2$ was generated along each media channel (Fig. 2). This gradient was confirmed by measurements using oxygen sensing films [7]. In addition, in cases where the same gas mixture containing 1%, 2%, 3%, or 21% O$_2$ was supplied to both gas channels, uniform oxygen environments of 1.3%, 2.3%, 3.3%, or 21% O$_2$ were generated in the media channels.

B. Cellular Experiments

The *Dd* cells (strain Ax2) were provided by National BioResource Project Cellular slime molds (NBRP Nenkin, Japan). The cells were cultured axenically with HL5 medium (Formedium, UK) on cell culture dishes at 22°C as amebic cells. After the cells were harvested from the culture dishes, they were introduced into the media channels in the microfluidic device at 100, 200, or 400 cells/mm^2 with the same HL5 medium, and incubated for 20 min to adhere to the bottom surface of the media channels. The device was then placed on a stage (TP-CHSQ-C, TOKAI HIT, Japan) controlled at 22°C, which was mounted on a microscope (IX83, Olympus, Japan). Gas mixtures containing 0% and 21% O$_2$ were supplied to the left and right gas channels, respectively, to generate an oxygen gradient along each media channel. Note that the *x*-direction is the direction in which the oxygen concentration becomes higher in the case that an oxygen concentration gradient was generated, and the *y*-direction is perpendicular to it. Alternatively, a gas mixture containing 1%, 2%, 3%, or 21% O$_2$ was supplied to both gas channels to generate a uniform oxygen concentration in the media channels. The gas flow rate in each gas channel was set at 30 ml/min. Time-lapse imaging was started just after the gas mixtures were started to be supplied. Phase-contrast microscopic images of the media channels were obtained every 30 s for 4 h. Experiments were conducted with three devices for each condition.

C. Cell Tracking

Dd cells in sequential microscopic images were analyzed to measure their cellular dynamics. A region of interest (ROI) of 5 mm × 1 mm (1500×300 pixels) was set at the center of each media channel ($-2.5 \leq x \leq 2.5$ mm) (see right image in

Fig. 1). The number of cells and their positions were detected by analyzing the microscopic images with the open-source software ImageJ (National Institutes of Health, USA) with its built-in plugin, Find Maxima. In addition, individual trajectories of the cell motions were obtained by tracking the cells using MATLAB (MathWorks, USA) with a squared-displacement minimization algorithm [10]. The raw and absolute values of the cell displacements per minute were calculated, and they were respectively averaged in each small region created by dividing the ROI at widths of 100 μm in the *x*-direction. Moreover, the change in the number of cells in each small region was calculated.
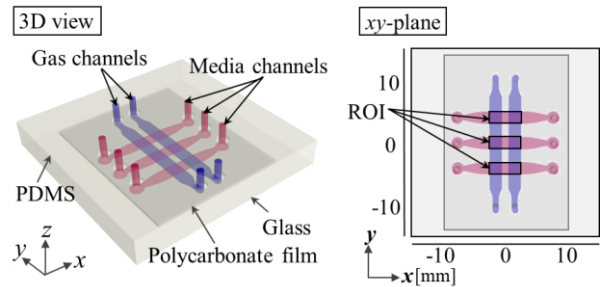

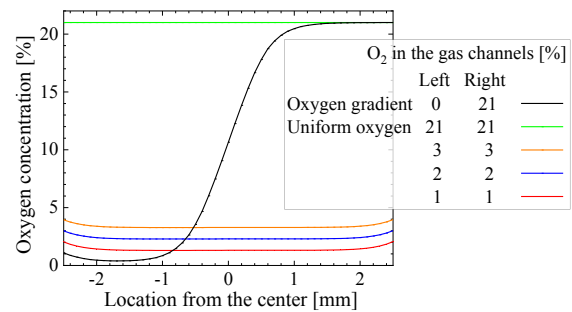Figure 1. Schematics of the developed microfluidic device.

Figure 2. Oxygen concentration profiles along the media channel.

III. RESULTS

A. Migration of D. Discoideum under an Oxygen Concentration Gradient (Aerotaxis)

Under the oxygen concentration gradient from 0.4% to 21% O$_2$, the *Dd* cells on the hypoxic side (left-hand side in the media channel) showed a different migration tendency compared with those on the normoxic side. On the hypoxic side, the *Dd* cells tended to migrate toward the normoxic side, and the cell density was decreased as time progressed (Fig. 3). A directionality of migration in the *x*-direction along the oxygen concentration gradient was observed, whereas there was no directionality in the *y*-direction (Fig. 4(a)). The average displacement of all cells in 1 min indicated that, under a hypoxic environment below a certain oxygen concentration, *Dd* cells respond to the oxygen concentration gradient and migrate toward a region with a higher oxygen concentration. A negative-to-positive change of displacement in the *x*-direction was observed at $x = -1.6$ mm, corresponding to the change of oxygen concentration gradient over the location with the lowest oxygen concentration. In addition, the average absolute value of displacement in 1 min was higher on the hypoxic side than on the normoxic side (Fig. 4(b)). Therefore, the migration speed was increased by the low oxygen concentration. Compared with the oxygen concentration

profiles in the device, this suggested that *Dd* change their migration under a hypoxic environment with an oxygen concentration of 2% or lower.
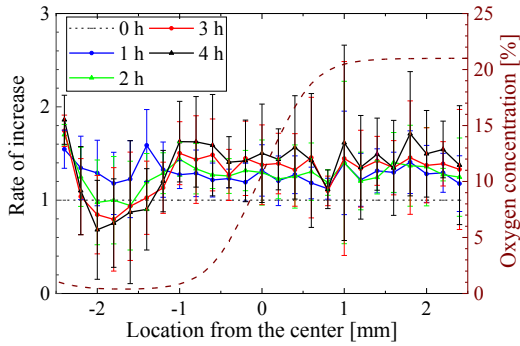

Figure 3. Increased rate of cell density under an oxygen concentration gradient from 0.4% O_2 to 21% O_2. Cell density at 0 h was 400 cells/mm². The error bars show the standard deviation of independent experiments ($n = 3$).
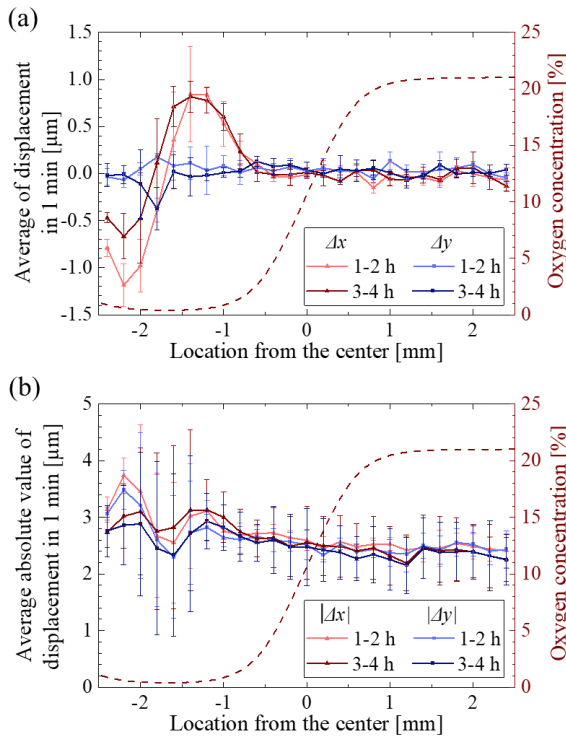

Figure 4. The *x* and *y*-directional displacements of the cells in 1 min under an oxygen concentration gradient from 0.4% O_2 to 21% O_2 between 1 h and 2 h, or 3h and 4h after the experiment was started. (a) Average of displacement in each region and (b) average of its absolute value. Cell density at 0 h was 400 cells/mm². The error bars show the standard deviation of independent experiments ($n = 3$).

It has been reported that various cellular dynamics of eukaryotic cells depend on cell density [11, 12]. Several behaviors of *Dd*, such as cell aggregation [13] and cell differentiation [14], cell motility [15, 16] and colony spreading [17] are also known to be cell density-dependent. Hence, we investigated whether the directional migration of *Dd* cells under the oxygen concentration gradient varied with the cell density by changing the initial cell density. As a result, regardless of cell density, the same tendency with an increased velocity of *Dd* cell toward a higher oxygen region from a hypoxic region was observed (Fig. 5).
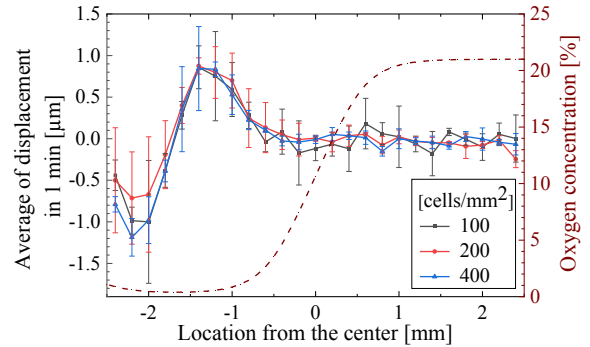

Figure 5. Comparison of experimental results with different initial cell densities. The *x*-directional displacement of the cells in 1 min under an oxygen concentration gradient from 0.4% O_2 to 21% O_2 between 1 h and 2 h after the experiment was started. The error bars show the standard deviation of independent experiments ($n = 3$).

B. Oxygen Concentration Dependence of Migration Velocity of D. Discoideum (Aerokinesis)

Considering the changes in the aerotactic behaviors of *Dd* cells on the hypoxic side under the oxygen concentration gradient, the migratory behaviors under uniform oxygen environments were measured to further investigate how *Dd* cell migration changes by oxygen concentration. The displacement of the *Dd* cells was drastically changed by the oxygen concentration (Fig. 6). Notably, the hypoxic environment generated by supplying a gas mixture with 1% O_2 significantly increased cell migration compared to the environments generated by supplying gas mixtures with 3% or higher O_2, even without an oxygen concentration gradient. This suggested that *Dd* cells increase migration velocity in response to hypoxic stress below a certain threshold of a few percent O_2. The increases of cell migration under the hypoxic conditions were similar to the results observed under the oxygen concentration gradient, but they were further pronounced under the severe oxygen condition (Fig. 7). At the location with 1.3% O_2 in the oxygen concentration gradient, the migration velocity was much lower than that under the uniform oxygen environment with the same oxygen concentration, though it was slightly increased compared to the normoxic side. Although the possibility of uncertain errors due to convection inside the device caused by physical vibration during imaging should be considered, the migration velocity observed under the uniform hypoxic environment with 1.3% O_2 was comparable to that at the location with 0.8% O_2 under the oxygen concentration gradient. Cell migration under the oxygen concentration gradient gradually attenuated as the oxygen concentration increased above 0.8% O_2.

IV. DISCUSSION

Dd sense an oxygen concentration gradient and migrate toward a region with a higher oxygen concentration under a hypoxic environment lower than 2% O_2. At the same time, they increase the migration velocity due to hypoxia itself. In this study, by developing a microfluidic device to conduct cellular experiments with *Dd*, we confirmed that both aerotaxis and aerokinesis of *Dd* cells are simultaneously induced in a hypoxic microenvironment with oxygen below a specific concentration [7]. We showed here for the first time that aerotaxis observed under the oxygen concentration gradient was not dependent on cell density. However, this does

not necessarily mean that the cell-cell interactions of *Dd* are not affected by the oxygen environment. Reportedly, a fold-change detection, which is a characteristic type of signal transduction in mammalian cells [18, 19], is also found in *Dd*, and the cell-cell signaling is partly independent of cell density [20]. Hence, it is necessary to carefully investigate the cell-cell interactions of *Dd* under different oxygen conditions. Furthermore, we compare for the first time cell migration under various uniform oxygen concentrations and an oxygen concentration gradient. It suggests that the aerotaxis does not depend simply on aerokinesis, which is an activated migratory behavior under low oxygen concentrations. The presence of an oxygen concentration gradient could have some effect on the oxygen sensitivity of cells. It might slow down aerokinesis, as the individual cells migrate and are exposed to a variation in oxygen concentration. In future work, we will measure aerotaxis and aerokinesis of *Dd* in more detail and investigate the mechanisms of oxygen-sensing and intracellular signal transduction.
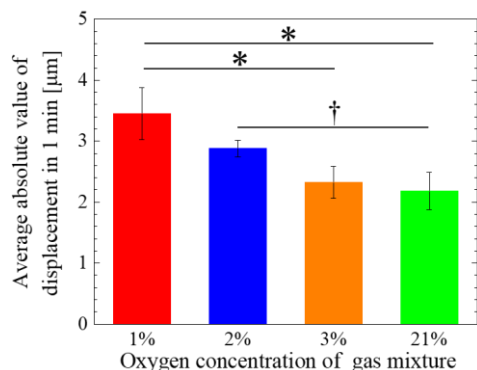

Figure 6. Comparison of the *x*-directional displacement of cells in 1 min under uniform oxygen concentrations between 1 h and 2 h after the experiment was started. Significant changes in cell displacement by oxygen concentration were assessed by 1-way ANOVA followed by Tukey's *post hoc* test for multiple comparisons. †$P < 0.1$; *$P < 0.05$. The error bars show the standard deviation of independent experiments ($n = 3$).
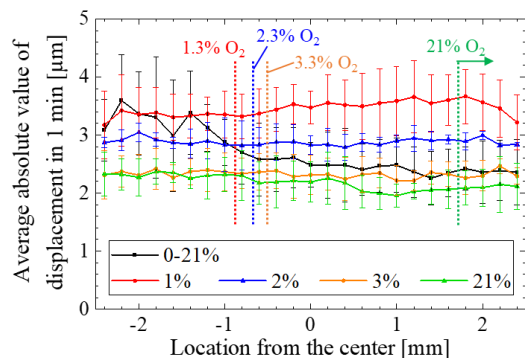

Figure 7. Comparison of the *x*-directional displacements of cells in 1 min under uniform oxygen concentrations and an oxygen concentration gradient between 1 h and 2 h after the experiment was started. The error bars show the standard deviation of independent experiments ($n = 3$). The dotted lines in the graph indicate the computed oxygen concentration under the oxygen concentration gradient.

ACKNOWLEDGMENT

REFERENCES

[1] P. Vaupel, K. Schlenger, C. Knoop, and M. Höckel, "Oxygenation of human tumors: evaluation of tissue oxygen distribution in breast cancers by computerized O_2 tension measurements," *Cancer Research*, vol. 51, no. 12, pp. 3316-3322, 1991.

[2] B. L. Krock, N. Skuli, and M. C. Simon, "Hypoxia-induced angiogenesis: good and evil," *Genes & Cancer*, vol. 2, no. 12, pp. 1117-1133, 2011.

[3] C. Murdoch, M. Muthana, and C. E. Lewis, "Hypoxia regulates macrophage functions in inflammation," *The Journal of Immunology*, vol. 175, no. 10, pp. 6257-6263, 2005.

[4] S. J. Annesley and P. R. Fisher, "*Dictyostelium discoideum*—a model for many reasons," *Molecular and Cellular Biochemistry*, vol. 329, no. 1-2, pp. 73-91, 2009.

[5] R. S. Williams *et al.*, "Towards a molecular understanding of human diseases using *Dictyostelium discoideum*," *Trends in Molecular Medicine*, vol. 12, no. 9, pp. 415-424, 2006.

[6] P. N. Devreotes and S. H. Zigmond, "Chemotaxis in eukaryotic cells: a focus on leukocytes and *Dictyostelium*," *Annual Review of Cell Biology*, vol. 4, no. 1, pp. 649-686, 1988.

[7] O. Cochet-Escartin *et al.*, "Hypoxia triggers collective aerotactic migration in *Dictyostelium discoideum*," *eLife*, (in press).

[8] C. M. West, Z. A. Wang, and H. van der Wel, "A cytoplasmic prolyl hydroxylation and glycosylation pathway modifies Skp1 and regulates O2-dependent development in Dictyostelium," (in eng), *Biochimica et biophysica acta*, vol. 1800, no. 2, pp. 160-171, 2010/02// 2010, doi: 10.1016/j.bbagen.2009.11.006.

[9] R. Koens *et al.*, "Microfluidic platform for three-dimensional cell culture under spatiotemporal heterogeneity of oxygen tension," *APL Bioengineering*, vol. 4, no. 1, p. 11, 2020.

[10] D. Blair and E. Dufresne. "The Matlab Particle Tracking Code Repository." (accessed Mar. 30, 2021).

[11] A. Tremel *et al.*, "Cell migration and proliferation during monolayer formation and wound healing," *Chemical Engineering Science*, vol. 64, no. 2, pp. 247-253, 2009.

[12] P. K. Shah *et al.*, "Human monocyte-derived macrophages induce collagen breakdown in fibrous caps of atherosclerotic plaques. Potential role of matrix-degrading metalloproteinases and implications for plaque rupture," *Circulation*, vol. 92, no. 6, pp. 1565-1569, 1995.

[13] B. Wang and A. Kuspa, "*Dictyostelium* development in the absence of cAMP," *Science*, vol. 277, no. 5323, pp. 251-254, 1997.

[14] Y. Hashimoto, M. Cohen, and A. Robertson, "Cell density dependence of the aggregation characteristics of the cellular slime mould *Dictyostelium discoideum*," *Journal of cell science*, vol. 19, no. 1, pp. 215-229, 1975.

[15] L. Golé, C. Rivière, Y. Hayakawa, and J.-P. Rieu, "A quorum-sensing factor in vegetative *Dictyostelium discoideum* cells revealed by quantitative migration analysis," *PLOS ONE*, vol. 6, no. 11, p. e26901, 2011.

[16] J. d'Alessandro, L. Mas, L. Aubry, J.-P. Rieu, C. Rivière, and C. Anjard, "Collective regulation of cell motility using an accurate density-sensing system," *Journal of The Royal Society Interface*, vol. 15, no. 140, p. 20180006, 2018.

[17] J. d'Alessandro *et al.*, "Contact enhancement of locomotion in spreading cell colonies," *Nature Physics*, vol. 13, no. 10, pp. 999-1005, 2017.

[18] C. Cohen-Saidon, A. A. Cohen, A. Sigal, Y. Liron, and U. Alon, "Dynamics and variability of ERK2 response to EGF in individual living cells," *Molecular Cell*, vol. 36, no. 5, pp. 885-893, 2009.

[19] L. Goentoro and M. W. Kirschner, "Evidence that fold-change, and not absolute level, of β-catenin dictates Wnt signaling," *Molecular Cell*, vol. 36, no. 5, pp. 872-884, 2009.

[20] K. Kamino, Y. Kondo, A. Nakajima, M. Honda-Kitahara, K. Kaneko, and S. Sawai, "Fold-change detection and scale invariance of cell–cell signaling in social amoeba," *Proceedings of the National Academy of Sciences*, vol. 114, no. 21, pp. E4149-E4157, 2017